The Hybrid Incompatibility Genes *Lhr* and *Hmr* Are Required for Sister Chromatid Detachment During Anaphase but Not for Centromere Function

Jacob A. Blum,*[,1] Silvia Bonaccorsi,*[,1] Marta Marzullo,* Valeria Palumbo,* Yukiko M. Yamashita,[†] Daniel A. Barbash,[‡,2] and Maurizio Gatti*[,§,2]

*Dipartimento di Biologia e Biotecnologie "C. Darwin," Sapienza, Università di Roma, 00185 Rome, Italy, [†]Life Sciences Institute, Department of Cell and Developmental Biology, Howard Hughes Medical Institute, University of Michigan, Ann Arbor, Michigan 48109, [‡]Department of Molecular Biology and Genetics, Cornell University, Ithaca, New York 14853, and [§]Istituto di Biologia e Patologia Molecolari (IBPM) del CNR, 00185 Rome, Italy

ORCID IDs: 0000-3001-5194-1765 (S.B.); 0000-0001-7229-1693 (M.M.); 0000-0001-5541-0216 (Y.M.Y.); 0000-0003-3777-300X (M.G.)

ABSTRACT Crosses between *Drosophila melanogaster* females and *Drosophila simulans* males produce hybrid sons that die at the larval stage. This hybrid lethality is suppressed by loss-of-function mutations in the *D. melanogaster Hybrid male rescue* (*Hmr*) or in the *D. simulans Lethal hybrid rescue* (*Lhr*) genes. Previous studies have shown that Hmr and Lhr interact with heterochromatin proteins and suppress expression of transposable elements within *D. melanogaster*. It also has been proposed that Hmr and Lhr function at the centromere. We examined mitotic divisions in larval brains from *Hmr* and *Lhr* single mutants and *Hmr*; *Lhr* double mutants in *D. melanogaster*. In none of the mutants did we observe defects in metaphase chromosome alignment or hyperploid cells, which are hallmarks of centromere or kinetochore dysfunction. In addition, we found that Hmr-HA and Lhr-HA do not colocalize with centromeres either during interphase or mitotic division. However, all mutants displayed anaphase bridges and chromosome aberrations resulting from the breakage of these bridges, predominantly at the euchromatin–heterochromatin junction. The few dividing cells present in hybrid males showed fuzzy and irregularly condensed chromosomes with unresolved sister chromatids. Despite this defect in condensation, chromosomes in hybrids managed to align on the metaphase plate and undergo anaphase. We conclude that there is no evidence for a centromeric function of Hmr and Lhr within *D. melanogaster* nor for a centromere defect causing hybrid lethality. Instead, we find that *Hmr* and *Lhr* are required in *D. melanogaster* for detachment of sister chromatids during anaphase.

KEYWORDS Lhr; Hmr; chromosome aberrations; anaphase; sister chromatid separation; interspecific hybrids; *Drosophila*

THE reduced fertility and viability of interspecific hybrids are widely observed causes of reproductive isolation that contribute to speciation. According to the classical Dobzhansky-Muller (D-M) model of hybrid incompatibility (HI), two or more loci that had independently diverged in nascent species can lead to deleterious HI effects when combined in interspecific hybrids. Although the D-M model is generally accepted, and numerous HI genes have been identified, the cytological and molecular mechanisms underlying HI are still poorly understood (reviewed in Presgraves 2010; Maheshwari and Barbash 2011).

Hybrids produced with *Drosophila melanogaster* offer strong opportunities to investigate mechanisms that cause HI (Barbash 2010). Crosses between *D. melanogaster* females and *Drosophila simulans* males produce viable but sterile females and no males, which die at the larval stage. This hybrid lethality is suppressed by loss of function mutations in the *D. melanogaster Hybrid male rescue* (*Hmr*) gene or in the *D. simulans Lethal hybrid rescue* (*Lhr*) gene (Maheshwari and Barbash 2011). The hybrid phenotype of these mutations indicates that hybrid lethality is caused by the wild-type alleles of these genes, which are therefore functioning as gain-of-function mutations in the hybrid background. Hybrid male

doi: https://doi.org/10.1534/genetics.117.300390
Manuscript received August 18, 2017; accepted for publication October 13, 2017; published Early Online October 18, 2017.
Supplemental material is available online at www.genetics.org/lookup/suppl/doi:10.1534/genetics.117.300390/-/DC1.
[1]These authors contributed equally to this work.
[2]Corresponding authors: Dipartimento di Biologia e Biotecnologie "C. Darwin," Sapienza, Università di Roma, Piazzale Aldo Moro, 5, 00185 Rome, Italy. E-mail: maurizio.gatti@uniroma1.it and; Department of Molecular Biology and Genetics, Cornell University, Ithaca, New York 14853. E-mail: barbash@cornell.edu

larvae from crosses between *D. melanogaster* females and *D. simulans* males die prior to pupal differentiation, and exhibit small brains and an almost complete absence of imaginal discs. Most cells in the brains of these larvae appear to be arrested either in G1 or G2, and the few dividing cells display defects in chromosome morphology (Orr *et al.* 1997; Bolkan *et al.* 2007).

A crucial step to elucidate how the interaction of *Hmr* and *Lhr* leads to hybrid lethality is to understand first their biological roles in each of the two species. Studies carried out in *D. melanogaster* have shown that neither *Hmr* nor the ortholog of *D. simulans Lhr* (henceforth designated *Lhr* without specifying that it is the *D. melanogaster* gene) is an essential gene. Flies homozygous for null mutations in either *Hmr* or *Lhr* are viable, but have reduced female fertility (Aruna *et al.* 2009; Satyaki *et al.* 2014).

The Hmr and Lhr proteins are enriched in the heterochromatin. In interphase embryonic cells, both proteins largely colocalize with the heterochromatin markers HP1a and H3K9me2 (histone H3 dimethylated at K9) (Maheshwari and Barbash 2012; Satyaki *et al.* 2014). In polytene chromosomes, Hmr and Lhr are enriched in both the α- and β-heterochromatin of the chromocenter, in a few euchromatic bands, and at the telomeres (Thomae *et al.* 2013; Satyaki *et al.* 2014). α-Heterochromatin occupies a small area in the middle of the chromocenter and contains mitotic heterochromatin and satellite DNAs, which are severely under-replicated in polytene chromosomes. α-Heterochromatin is connected to the euchromatic chromosome arms by β-heterochromatin, which is enriched in diverse arrays of unique and repetitive DNA sequences but not in satellite DNA (Miklos and Cotsell 1990; Gatti and Pimpinelli 1992). Consistent with their heterochromatic and telomeric localizations, Hmr and Lhr associate with heterochromatin protein 1a (HP1a), and Hmr and Lhr interact with each other in the yeast two-hybrid assay, suggesting that the three proteins are part of a complex within which Hmr and Lhr interact directly (Thomae *et al.* 2013; Alekseyenko *et al.* 2014; Satyaki *et al.* 2014).

Thomae *et al.* (2013) proposed that Hmr and Lhr are centromere proteins. This suggestion was based on three main findings. They reported that, in interphase imaginal disc cells, Hmr and Lhr localize to heterochromatic regions that are partially coincident with those immunostained for the centromere markers Cid and Cenp-C (Thomae *et al.* 2013). Using tandem copurification experiments followed by mass spectrometry, and additional coprecipitation experiments, they identified 60 Hmr-Lhr interacting proteins, including Cenp-C, which is a centromere-specific component (Heeger *et al.* 2005), as well as HP1 and HP6/Umbrea, which are enriched in centromeric heterochromatin (Greil *et al.* 2007; Ross *et al.* 2013). They also observed lagging chromosomes in anaphases of Hmr- and Lhr-depleted cells (Thomae *et al.* 2013). Several aspects of their report, however, leave open alternative interpretations about Hmr and Lhr function. First, many of the copurifying proteins they identified have noncentromeric functions. For example, HP1a and HP6/Umbrea localize also in noncentromeric heterochromatic regions and at telomeres, and HP1a has been shown to prevent telomere fusion in somatic cells (Fanti *et al.* 1998; Joppich *et al.* 2009; Vermaak and Malik 2009; Elgin and Reuter 2013). In addition, three proteins that copurify with Hmr-Lhr (Ver, Moi, and CG30007/Tea) are components of the *Drosophila* telomere-capping complex, identified by lethal mutations that cause frequent telomeric fusions (TFs) in larval brain cells (Raffa *et al.* 2009, 2010; Zhang *et al.* 2016; Cicconi *et al.* 2017). Thus, the interactions between Hmr-Lhr and proteins such as HP1a, HP6/Umbrea do not necessarily occur at centromeres. Second, centromeric localization of Hmr and Lhr was not observed in metaphase chromosomes (Thomae *et al.* 2013), nor did Lhr colocalize with Cid in embryonic interphase nuclei (Maheshwari and Barbash 2012). Third, the centromeric role of Hmr and Lhr proposed by Thomae *et al.* 2013 is unclear, because they found that loss of neither Hmr nor Lhr affects centromeric localization of essential centromere/kinetochore components including Cid, Cenp-C, Ndc80, Incenp, Polo, and Rod.

We therefore investigated here, using extensive cytological analysis of larval brain cells, whether *Hmr* and *Lhr* affect centromere function, or potentially a different aspect of chromosome segregation. We found that these mutants exhibit very low levels of TFs. However, they displayed relatively high frequencies of incomplete chromosome breaks, namely broken chromosomes without the corresponding fragment or complete chromosome complements plus an extra acentric fragment. These two types of chromosome aberrations (CABs) are likely generated during anaphase (Mengoli *et al.* 2014). Notably, we did not observe aneuploid cells with unbroken chromosomes in either *Hmr* or *Lhr* mutant brains or failure of the centromeres to separate and move toward the poles. In addition, immunolocalization experiments in larval brain cells showed that neither Hmr-HA nor Lhr-HA colocalizes with the centromeres throughout the cell cycle. Thus, our results strongly suggest that the Hmr-Lhr complex is not required for centromere or kinetochore function.

Materials and Methods

Drosophila strains and crosses

Hmr^{3}, also called $Hmr^{EY12237}$, carries a {EPgy2} insertion within the gene, and is a null allele by genetic criteria (Aruna *et al.* 2009). Lhr^{KO}, generated by a targeted w^{+} insertion within the gene, carries a 26-bp deletion of the coding sequence, and is also a null mutation (Satyaki *et al.* 2014). Both Hmr^{3} and Lhr^{KO} were maintained as homozygous stocks, which were used to collect larvae for cytological analyses. To generate the double mutant, we crossed Hmr^{3}/Y; $Lhr^{KO}/CyO\text{-}Tb$ males to $Hmr^{3}/FM7\text{-}Tb$; $Lhr^{KO}/CyO\text{-}Tb$ females. The offspring from these crosses, left to mate for a few generations, lost the balancers and became homozygous for both Hmr^{3} and Lhr^{KO}. Larvae from this homozygous stock were

used for the analysis of chromosome integrity and mitotic division. The *FM7-Tb* and *CyO-Tb* balancers, which carry the dominant larval marker *Tb*, are described in Lattao *et al.* (2011).

Chromosome cytology

To analyze CABs in metaphases, brains from third-instar larvae were dissected in saline (NaCl 0.7%) and incubated for 1 hr in saline with colchicine (10^{-5} M); brains were then treated for 8 min with hypotonic solution (0.5% Na citrate), and squashed in 45% acetic acid under a 20 × 20 mm coverslip. To analyze anaphases and assess mitotic parameters, larval brains were dissected in saline, and squashed in 45% acetic acid directly without colchicine and hypotonic pretreatment. Both types of chromosome squashes were frozen in liquid nitrogen; after flipping off the coverslip slides were air-dried and then mounted in Vectashield H-1200 (Vector Laboratories, Burlingame, CA) with DAPI (4,6 diamidino-2-phenylindole) to stain the chromosomes and reduce fluorescence fading.

To calculate the mitotic index (MI) and the frequency of anaphases, we scored DAPI-stained brain squashes for the presence of mitotic figures. MI is the average number of mitotic figures per optic field, while the frequency of anaphases is the ratio between the number of anaphases and the total number of mitotic figures observed (Gatti and Goldberg 1991).

Subcellular localization of Hmr-HA and Lhr-HA

The Hmr-HA and Lhr-HA transgenes were described previously (Maheshwari and Barbash 2012; Satyaki *et al.* 2014). To examine their localization in larval brain cells, brains from crawling third instar larvae were dissected in PBS, transferred to 0.5% Na citrate for 10–20 min, and transferred onto a 25 μl drop of fixative (4% formaldehyde in PBST). While being fixed (for 4 min), the brains were manually dissected into smaller pieces to ensure better spread of cells. After fixation, the tissues were squashed and frozen in liquid nitrogen. After flipping off the coverslips, slides were washed in PBS for ~1 hr, and incubated overnight with primary antibodies (chicken anti-Cid; 1:500, generated at Covance against the peptide AKRAPRPSANNSKSPNDD; and rat anti-HA, 1:100; Sigma-Aldrich) in 3% BSA in PBST at 4°. We regularly use the anti-HA antibody to stain other HA-tagged proteins, and we have never observed cross reaction/background staining. The slides were washed in PBS for ~1 hr and then incubated overnight with secondary antibodies (anti-Chicken AlexaFluor-488, anti-rat AlexaFluor-568) at 4°. The slides were washed for ~1 hr and mounted in Vectashield H-1200 (Vector Laboratories) with DAPI.

Mitotic chromosome and spindle immunostaining

For immunostaining with anti-tubulin and anti-phosphohistone H3 (PH3) antibodies, brains from third instar larvae were dissected in saline, fixed in formaldehyde, and squashed as described in Bonaccorsi *et al.* (2000). For PH3 immunostaining, preparations were incubated overnight at 4° with a rabbit anti-PH3 (Ser10) antibody (Upstate Biotechnology, Lake Placid, NY) diluted 1:100 in PBS with 5% goat serum. The anti-PH3 antibody was detected by a 1-hr incubation at room temperature with an Alexa 555-conjugated anti-rabbit IgG (Molecular Probes, Eugene, OR) diluted 1:300 in PBS. For tubulin immunostaining, slides were incubated overnight at 4° with an anti-α-tubulin monoclonal (DM1A diluted 1:100; Sigma), which was detected by a 1-hr incubation at room temperature with FITC-conjugated anti-mouse (1:100; Jackson Laboratories, Bar Harbor, ME) diluted in PBS. All cytological preparations were mounted in Vectashield H-1200 with DAPI, and images were captured with a CoolSnap HQ CCD camera (Photometrics, Tucson, AZ) connected to a Zeiss Axioplan fluorescence microscope equipped with an HBO 100 W mercury lamp.

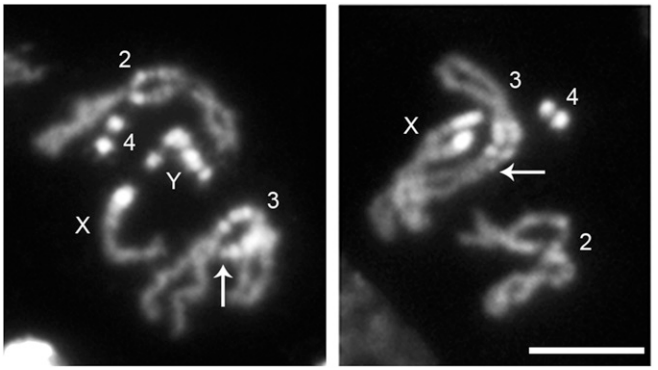

Figure 1 Lhr^{KO} mutants exhibit a minor difference in the most distal fluorescent bands of the 3R heterochromatin (arrows) compared to wild type Oregon R flies. The cells shown are male (left) and female (right) late prophases from F1 third instar larvae generated by crosses between Oregon R females and Lhr^{KO} mutant males. Bar, 5 μm.

Data availability

Fly strains are available from the authors upon request.

Results

Structure of chromosomes in Hmr and Lhr mutant stocks

Because both *Hmr* and *Lhr* have been implicated in the maintenance of heterochromatin, we first examined the mitotic chromosomes of each mutant for the structure of the heterochromatic regions. This is an important control to exclude the possibility that the chromosome aberration phenotypes that we describe below are due to chromosomal abnormalities that pre-exist in the mutant stocks that we are using. We crossed mutant males with wild type Oregon-R females, and then examined the heterozygous progeny for the DAPI banding pattern of larval brain heterochromatin. In late prophase cells of these larval brains the Oregon-R chromosome is paired with its mutant homolog, facilitating a comparison between the heterochromatic regions. Because the Hoechst banding pattern of the Oregon-R heterochromatin (which is identical to that obtained with DAPI) has been carefully characterized (reviewed

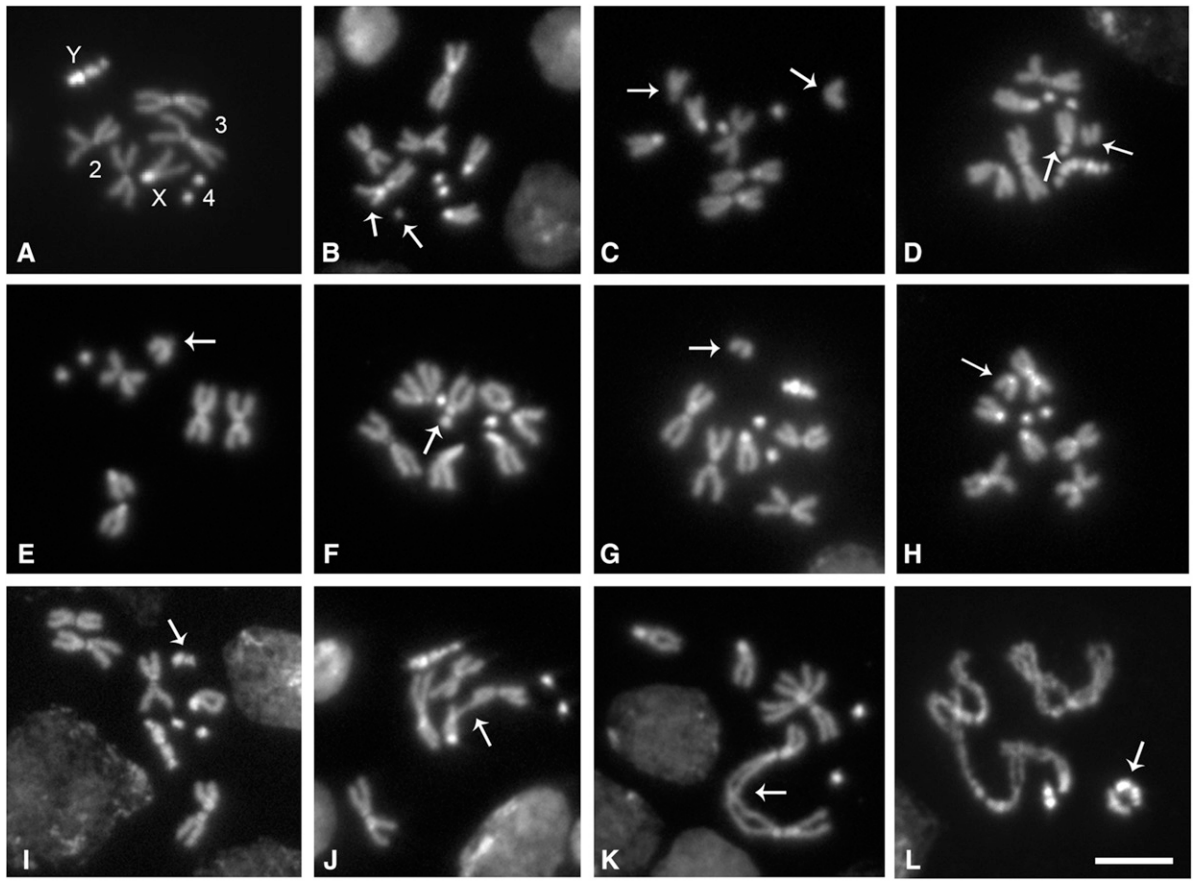

Figure 2 Examples of CABs observed in colchicine-treated metaphases from *Lhr* and *Hmr* mutants. (A) Male control metaphase; the third chromosomes are easily distinguished from the second chromosomes by the higher fluorescence of their pericentric heterochromatin. (B) Chromatid deletion (arrows). (C) Second chromosome ISOB in centric heterochromatin, probably at the euchromatin–heterochromatin (eu-het) junction (arrows). (D) Third chromosome ISOB at the eu-het junction (arrows). (E) Incomplete ISOB; a second chromosome (arrow) is broken within the heterochromatin or at the eu-het junction, but lacks the corresponding acentric fragment. (F) Incomplete ISOB; a third chromosome broken at the eu-het junction (arrow) lacking the corresponding acentric fragment. (G–I) Metaphases with complete chromosome complements and an additional euchromatic fragment (G; arrow), an additional autosomal arm broken in the heterochromatin (H, arrow), or an additional Y fragment (I, arrow). (J) TF involving single chromatids of the X and the second chromosome (arrow). (K) Double TF involving both sister chromatids of the two third chromosomes (arrow). (L) TF leading to a ring Y chromosome (arrow). Bar, 5 μm.

by Gatti and Pimpinelli 1992), this analysis permitted us to assess precisely whether the heterochromatic regions of the chromosomes from the Hmr^{3} and Lhr^{KO} stocks are different from those of Oregon-R wild type flies. We found that the heterochromatic regions of both mutants are virtually identical to those of Oregon-R (at least 50 cells from at least three brains were scored for each sample), with a minor difference in the most distal fluorescent bands of the 3R heterochromatin in Lhr^{KO} flies (Figure 1). Although the precise nature of this difference is not clear, it is highly unlikely to account for the range of CABs described below (Figure 2, Table 1, and Table 2).

Mutations in Hmr and Lhr cause CABs but not aneuploid cells in larval brains

To investigate the mitotic roles of *Hmr* and *Lhr*, we examined third-instar larval brains from Hmr^{3} and Lhr^{KO} homozygotes and from Hmr^{3}; Lhr^{KO} double homozygous mutants. The double mutant was viable and did not show any appreciable morphological phenotype. This observation suggests that the simultaneous loss of both Hmr and Lhr is equivalent to the loss of either single protein, consistent with the finding that the Hmr and Lhr proteins are mutually dependent for their stability (Thomae *et al.* 2013). We incubated brains in saline with colchicine for 1 hr before hypotonic treatment and fixation. Colchicine arrests mitotic cells in metaphase and hypotonic treatment results in chromosome spreading. Preparations obtained in this way allow unambiguous assessment of both CABs and TFs (Gatti and Goldberg 1991; Cenci *et al.* 1997). Examination of these preparations also allows detection of aneuploid cells. We classified as aneuploid cells only hyperploid figures showing a normal chromosome complement plus one or more additional unbroken chromosomes, all displaying the same degree of mitotic condensation; we did not consider hypoploid cells missing one or more chromosomes because they can occasionally be generated artifactually by the squashing procedure.

Table 1 Mutations in *Lhr* and *Hmr* cause CABs

Mutant, Sex	Number of Brains	Number of Cells	CD	ISOBs with F				ISOBs with no F				Extra F			E	TFs	H	CABs %	TFs %
				eu	Ah	X	Y	eu	Ah	X	Y	eu	Ah	Y					
Hmr^{3}, f	14	914	2	6	7	2	—	1	13	4	—	6	8	—	2	8	2	5.6	0.9
Hmr^{3}, m	12	920	1	9	7	4	2	1	15	1	3	2	4	3	1	6	3	5.8	0.7
Hmr^{3}/+, f	9	929	0	1	0	1	—	0	0	0	—	1	1	—	0	0	0	0.5	0
Lhr^{KO}, f	18	1404	6	4	14	5	—	2	19	6	—	7	10	—	0	6	2	5.2	0.4
Lhr^{KO}, m	12	1804	15	9	32	2	9	1	24	6	5	12	15	8	0	7	5	7.7	0.4
Lhr^{KO}/+, f	7	740	2	0	0	0	—	0	1	0	—	0	0	—	0	0	0	0.4	0
Lhr^{KO}/+, m	8	871	1	0	0	0	0	0	0	0	0	0	0	0	0	0	0	0.1	0
Double, f	20	2364	11	17	30	7	—	2	26	3	—	20	18	—	2	14	5	5.7	0.6
Double, m	23	2720	17	11	25	4	8	3	22	1	10	23	29	5	2	18	6	5.9	0.7

CABs were detected in colchicine-treated and hypotonically swollen metaphases of both females (f) and males (m). CD, chromatid deletions (breaks involving a single chromatid). ISOBs isochromatid breaks (both sister chromatids broken at the same location); F, acentric fragment (in ISOBs with F, both the centric and the acentric fragment are present; in ISOBs with no F, only the centric fragment is present; the extra F class includes cells with a complete chromosomal complement accompanied by an extra F). Ah, broken within autosomal heterochromatin; E, chromatid- or chromosome-type exchanges; TFs, telomeric fusions; H, hyperploid metaphases. Double, Hmr^{3}; Lhr^{KO} double homozygous mutant. The frequencies of CABs were calculated without taking into account cells with TFs and hyperploid cells; TF frequencies were calculated without taking into account hyperploid cells.

Examination of larval brain preparations form Hmr^{3} and Lhr^{KO} homozygous larvae and from Hmr^{3}; Lhr^{KO} double homozygous mutants revealed very similar patterns and frequencies of chromosome abnormalities (Figure 2 and Table 1). In single and double mutants ~5–8% of colchicine-arrested metaphases showed CABs, and TFs were found in ~0.4–0.9% of metaphases. The frequency of CABs in these mutants is >10-fold higher than that observed in Hmr^{3}/+ and Lhr^{KO}/+ heterozygotes (0.1–0.5%; Table 1) or previously observed in Oregon-R controls, all of which showed from 0.3 to 0.7% cells with CABs (Gatti *et al.* 1974; Gatti 1979; Benna *et al.* 2010; Marzio *et al.* 2014; Merigliano *et al.* 2017). The TF frequencies observed in Hmr^{3} and Lhr^{KO} mutants are very low, but are nonetheless a clear departure from normality, given that the TF frequency in control cells is virtually zero (Table 1).

Most CABs observed in the mutants were isochromatid breaks in which both sister chromatids are broken at the same location. Notably, >60% of these isochromatid breaks were incomplete; that is, they consisted either of a centric fragment without the corresponding acentric element, or of an acentric fragment associated with a normal chromosome complement (Figure 2). These incomplete isochromatid breaks (ISOBs) are rather rare in other mutants that exhibit CABs [*mei-9*, *mei-41* (ATR), *mus-102*, *mus-105*, *mus-109*, *tim2*, *dPdxk*, and *tws*], where they ranged from 2 to 5% of total isochromatid breaks (Gatti 1979; Benna *et al.* 2010; Marzio *et al.* 2014; Merigliano *et al.* 2017). Such ISOBs are in contrast very frequent in *Topoisomerase2* (*Top2*) mutants, where they are caused by the rupture of chromosome bridges generated during anaphase due to failure of sister chromatid decatenation (Mengoli *et al.* 2014). Although ISOBs and at least some complete isochromatid breaks observed in colchicine-arrested metaphases are likely to result from breaks generated during anaphase of the previous cell cycle (Figure 3), chromatid deletions (breaks involving only one of the two sister chromatids; see Figure 2 and Table 1) cannot be the outcome of anaphase defects, but rather must result from lesions produced during S or G2 phase. Thus, the low frequencies of chromatid deletions observed in *Lhr* and *Hmr* (~0.1–0.8%) are likely to reflect the presence of double-strand breaks, the type of DNA lesion that is thought to lead to chromosome breakage (Obe *et al.* 2002; Durante *et al.* 2013).

In both *Hmr* and *Lhr* mutants, >70% of all breaks are located in heterochromatin, or at the junction between euchromatin and heterochromatin (henceforth designated as heterochromatic breaks). In previous studies, mutants in *mei-9*, *mei-41*, and *mus-102*, and X-ray treated wild-type cells displayed 40–50% heterochromatic breaks, while mutants in *mus-105* and *mus-109* showed 18 and 81% heterochromatic breaks, respectively (Supplemental Material, Table S1). The proportion of breaks in the Y chromosome in males is also higher for *Hmr* and *Lhr* than any previous condition analyzed. It is likely that the high frequency of heterochromatic breaks observed in *Hmr* and *Lhr* mutants reflects a specific fragility of heterochromatin and euchromatin–heterochromatin junctions during anaphase, similar to that observed in *Top2* mutants (Mengoli *et al.* 2014). However, while in *Top2* mutants most ISOBs involve the Y chromosome and a distal heterochromatic region in the 3L arm (region h47), in *Hmr* and *Lhr* mutants isochromatid breaks involve the Y and both the second and the third chromosome heterochromatin (Table 1 and Table 2). Assessing isochromatid breaks within the X chromosome heterochromatin was difficult because breaks that separate

Table 2 Distribution of heterochromatic breaks among the major autosomes

Mutant, Sex	Total Breaks	Second Chromosome Heterochromatin	Third Chromosome Heterochromatin
Hmr^{3}, f and m	47	27	20
Lhr^{KO}, f and m	63	38	25
Hmr^{3}; Lhr^{KO}, f and m	65	32	33

Observations were limited to metaphases allowing unambiguous recognition of the second and third chromosome. f, females; m, males.

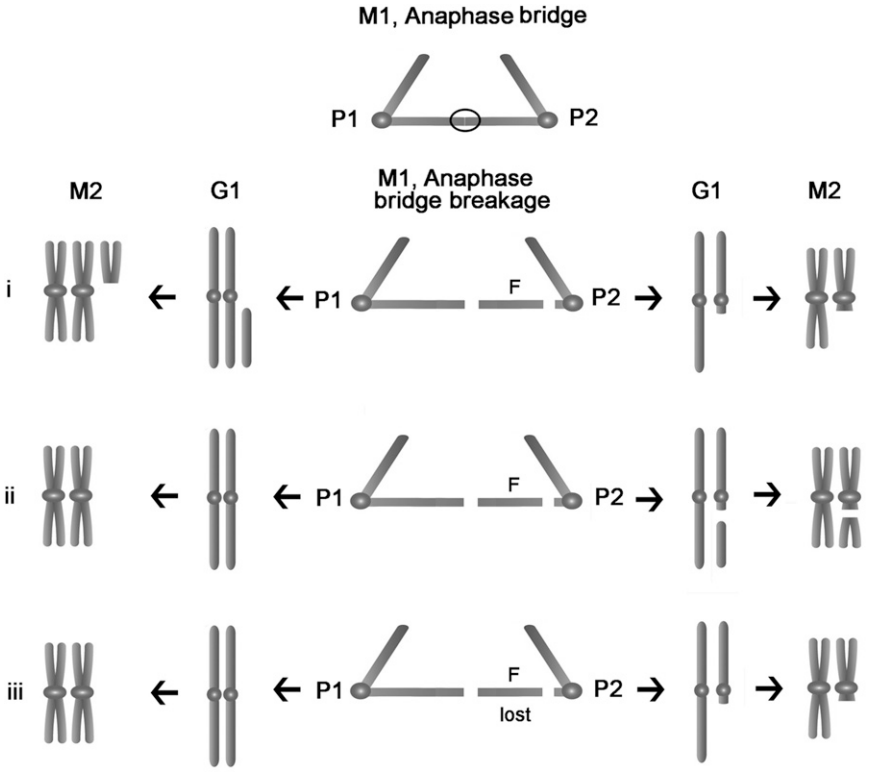

Figure 3 A model for the formation of ISOBs. The primary event leading to an incomplete ISOB is the formation of a chromatin bridge generated by a transient sister chromatid association during anaphase, represented by an ellipse. This association can be generated by failure to resolve aberrant sister chromatid cohesion or by tangles, such as those caused by mutations in the condensin genes (see *Discussion* for details on the possible origins of anaphase bridges). The anaphase drawing refers to the mitosis in which the anaphase bridge forms (M1), and depicts a single chromosome composed of a pair of sister chromatids; centromeres are represented by circles. G1 and metaphase 2 (M2) refer to the subsequent cell cycle, and show both homologous chromosomes, one of which segregated normally during the previous anaphase. The metaphase configurations are those observed in colchicine-treated cells of mutants that are shown in Figure 2. Stretching of the bridge during anaphase would result in the resolution of the sister chromatid association, and a rupture at the eu-het junction. This situation could have three possible outcomes: (i) the acentric fragment (F) segregates with the chromatid to which it was originally attached, giving rise to a telophase nucleus containing both homologous chromosomes plus an acentric element (at cell pole 1, P1), and to another nucleus containing only the centric element and no corresponding acentric fragment (at cell pole 2, P2). (ii) The acentric fragment segregates with its corresponding centric element producing a normal nucleus at P1 and a nucleus bearing a complete ISOB at P2. (iii) The acentric fragment is lost, leading to a normal telophase nucleus at P1 and to a nucleus containing a broken chromosome without the corresponding fragment at P2. This model describes the possible outcomes of a rupture at the eu-het junction but could also be extended to ruptures in the euchromatin.

the DAPI-bright from DAPI-dull region of X heterochromatin produce fragments that closely resemble a fourth chromosome and an autosomal arm, respectively.

In both the single and the double mutants, hyperploid cells were quite rare, ranging only from 0.2 to 0.3%. This is not due to a low survival rate or low division potential of hyperploid cells, because this type of cell is very frequent in *Drosophila* mutants defective in chromosome segregation. For example, mutants in the *zw10* gene that encodes a component of the spindle checkpoint machinery display 50–60% hyperploid cells (Smith *et al.* 1985; Williams *et al.* 1992). Similarly, mutants in the *mitch* gene that specifies a subunit of the Ndc80 kinetochore complex exhibit 43% hyperploid cells (Williams *et al.* 2007).

Analysis of cell division in noncolchicine-treated cells from Hmr and Lhr mutant brains reveals abnormal anaphases

To obtain insight into the mechanism leading to the incomplete CABs observed in colchicine treated cells, we examined mitotic division in mutant brains in the absence of colchicine or hypotonic treatment, in order to directly visualize anaphases. We first determined the MI and the frequencies of anaphases in Hmr^{3}; Lhr^{KO} double mutants, in which the function of the Hmr-Lhr complex should be eliminated completely. Hmr^{3}; Lhr^{KO} brains displayed a MI and a frequency of anaphases comparable to those observed in wild-type controls, suggesting that mutant cells progress through mitosis at the same rate as wild-type cells (Table 3).

We next examined anaphase figures in both *Hmr* and *Lhr* single mutants and *Hmr*; *Lhr* double mutants. We found that a substantial fraction of mutant anaphases (ranging from 11.9 to 16.5%; Figure 4 and Table 4) display chromosome bridges, bridges plus fragments, or acentric fragments, but no anaphases showed intact lagging chromosomes. These observations support the hypothesis that the incomplete aberrations shown in Figure 2 were generated by chromosome breakage occurring during a previous anaphase. The defective anaphases observed in *Hmr* and *Lhr* mutants are unlikely to be the outcome of TFs, as the TF frequency is ~20-fold lower than that of aberrant anaphases (Table 1).

Finally, we examined preparations fixed with formaldehyde and stained for tubulin and DNA, and counted the cells with prometaphase/metaphase spindles showing aligned or unaligned chromosomes. This analysis revealed no differences between wild type controls and mutant cells, suggesting that neither *Hmr* nor *Lhr* are required for formation of the metaphase plate (Figure 5 and Table 5).

Dynamic behavior of Hmr and Lhr during mitotic division

To gain further insight into the roles of Hmr and Lhr, we stained brain preparations from larvae that express either Hmr-HA or Lhr-HA with anti-HA and anti-Cid (a centromere marker homologous to Cenp-A) antibodies. We found that Hmr and Lhr exhibit very similar dynamic behaviors in both

Table 3 *Hmr; Lhr* double mutants exhibit normal mitotic parameters

Genotype, Sex	Number of Fields	Prophases and Prometaphases	Metaphases	Anaphases	Divisions/fields (MI)	Anaphases (%)
WT control, f	180	292	40	72	2.2	14.8
WT control, m	172	304	54	62	2.4	17.8
Hmr^3; Lhr^{KO}, f	338	720	103	177	3.0	17.7
Hmr^3; Lhr^{KO}, m	261	540	68	116	2.8	16.0

Brains were fixed without colchicine or hypotonic treatment, squashed and stained with DAPI to visualize chromosomes.

male (Figure 6 and Figure 7) and female (Figure S1 and Figure S2) cells. In interphase cells, Lhr and Hmr showed similar localizations near, but not overlapping with, the DAPI-bright heterochromatin, and did not colocalize with Cid (Figure 6A, Figure 7A, Figure S1A, and Figure S2A). This localization pattern suggests that both proteins are enriched in heterochromatin regions that are not fluorescent after DAPI or Hoechst 33258 staining (see Gatti and Pimpinelli 1992, for a map of mitotic heterochromatin). In the sole very early prophase we were able to find, where only heterochromatin has started to condense and euchromatin is still diffuse, Lhr was clearly associated with heterochromatin, and concentrated in chromosomal regions that are not DAPI-bright (Figure 7B). Lhr was also associated with dully fluorescent heterochromatic regions in another early prophase, in which euchromatin was visible but poorly condensed (Figure S2B). In all other prophases stained for Lhr (nine male and 10 female prophases), Lhr was not associated with the chromosomes, and exhibited a diffuse nucleoplasmic localization (Figure 7C and Figure S2C). Hmr was dispersed within the nucleoplasm, and did not exhibit a clear accumulation in dully fluorescent heterochromatic regions of the chromosomes in all the five male and seven female prophases scored. We observed only an occasional Hmr accumulation at a small pericentromeric chromosomal region (Figure S1B) (likely 2R heterochromatin, based on its localization on metaphase chromosomes). However, none of the prophases stained for Hmr was a very early one, like that shown for Lhr in Figure 7B. Thus, we cannot exclude that Hmr remains associated with heterochromatin during the earliest stages of prophase, as Lhr does. Regardless of this possible small difference in behavior, however, our results strongly suggest that both Lhr and Hmr mostly dissociate from the chromosomes during early prophase.

Lhr was consistently dissociated from the chromosomes in prometaphase ($n = 14$) and metaphase ($n = 11$) cells (Figure 7D and Figure S2D). Hmr too was mostly dissociated from prometaphase and metaphase chromosomes (Figure 6, C and D and Figure S1, C and D), but in a fraction of the cells (4/12 in males, 12/28 in females), a small amount of Hmr was concentrated in a single nonfluorescent region of the 2R heterochromatin [region h42 according the heterochromatin map of Gatti and Pimpinelli (1992)], well separated from the centromeric region marked by Cid (Figure 6D and Figure S1C). Because this accumulation of Hmr in region h42 is seen in prophase (Figure S1B), it likely results from a remnant of Hmr that failed to dissociate from heterochromatin when cells enter mitosis. During anaphase, both Hmr and Lhr become incorporated again into heterochromatin (Figure 6E, $n = 6$; Figure 7, E and F, $n = 7$; S1E, $n = 11$; S2E, $n = 3$). In some early anaphases (3/7) Lhr was concentrated in regions distal to both the chromosomes and the Cid signals, which are likely to correspond to the spindle poles (Figure 7E). This observation raises the intriguing possibility that Lhr travels toward the spindle poles along the microtubules, so as to favor its recruitment

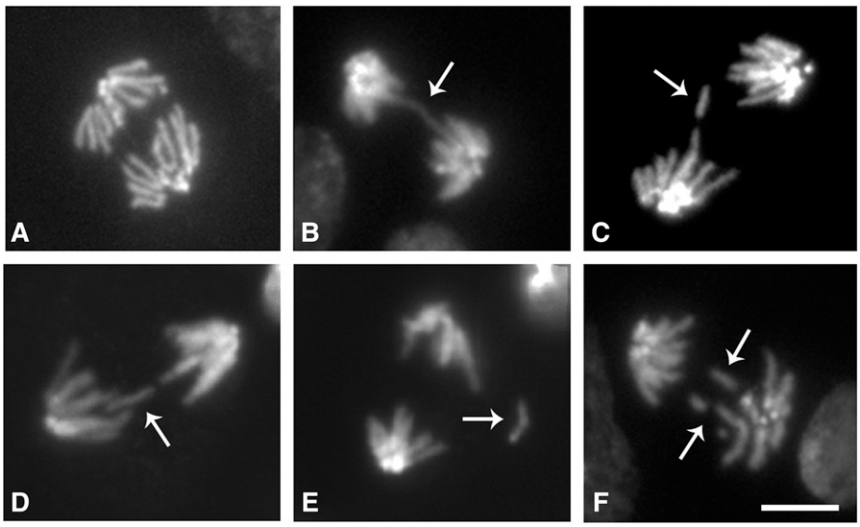

Figure 4 Examples of aberrant anaphases observed in *Lhr* and *Hmr* mutants. (A) Wild-type control anaphase. (B) Anaphase with bridge. (C and D) Anaphases with a broken bridge and a fragment. (E) Anaphase with a fragment. (F) Anaphase with fragments (arrows). Bar, 5μm.

Table 4 Anaphase defects in *Hmr* and *Lhr* mutants

Genotype, Sex	Number of Brains	Number of Anaphases	Bridge or Broken Bridge	Bridge and Fragment	Acentric Fragment	% Defective
WT control, f	7	104	1	0	1	1.9
WT control, m	8	115	2	0	0	1.7
Hmr^{3}, f	9	78	4	4	2	12.8
Hmr^{3}, m	9	116	7	4	6	14.7
Lhr^{KO}, f	8	101	8	2	2	11.9
Lhr^{KO}, m	19	326	29	10	7	14.1
Lhr^{KO}; Hmr^{3}, f	13	286	16	15	8	13.6
Lhr^{KO}; Hmr^{3}, m	11	237	19	14	6	16.5

by the pericentric heterochromatin. Finally, we note that, in both Hmr-HA- and Lhr-HA-expressing cells, the nonchromocentral regions of interphase nuclei were faintly stained, suggesting that, while the bulk of Hmr and Lhr is in the heterochromatin, small amounts of these proteins are associated with euchromatin.

In summary, these results show that Lhr and Hmr colocalize with the non-DAPI-bright heterochromatin, but not with the Cid-stained centromeres during interphase. Both Lhr and Hmr mostly dissociate from heterochromatin during prophase, and return to heterochromatin during anaphase. To explain the slightly different dynamic behaviors of Lhr and Hmr, we

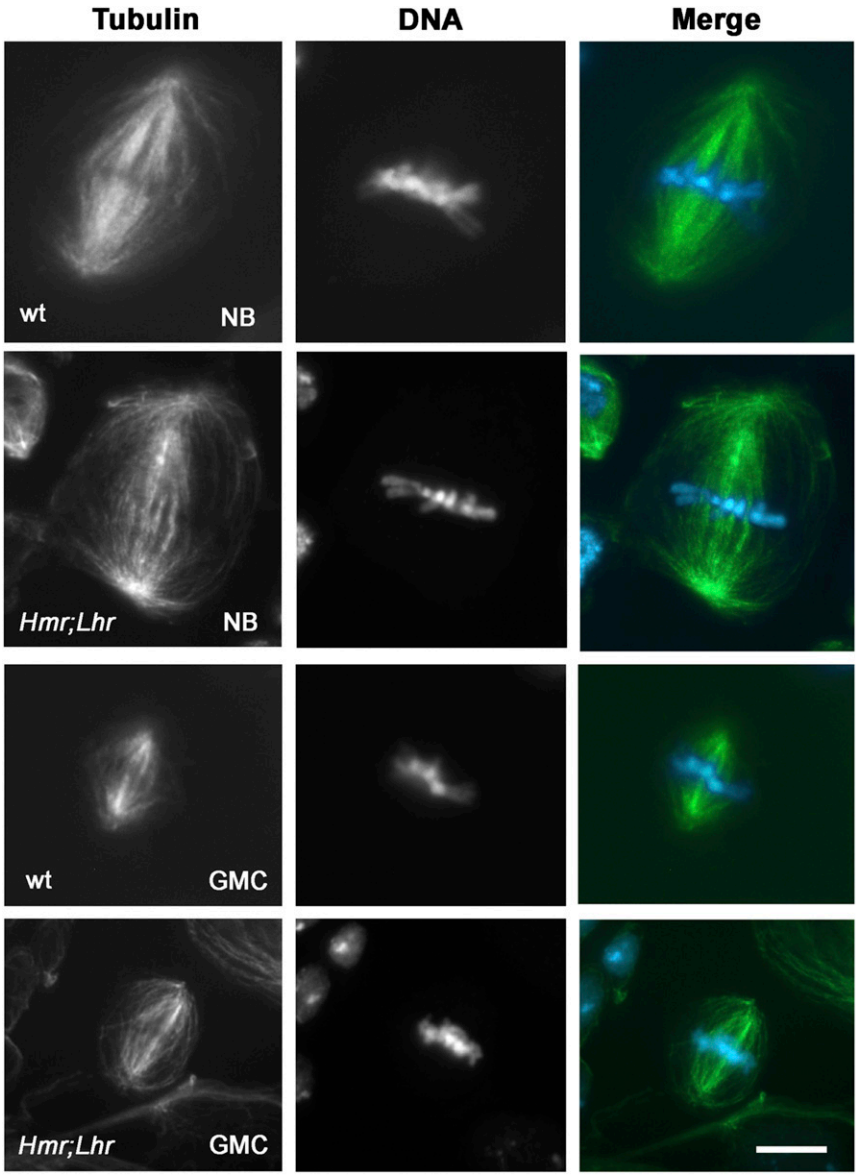

Figure 5 Examples of well-aligned metaphases observed in brains from wild type (wt, Oregon R) and *Hmr*; *Lhr* double homozygous mutants. NB, neuroblast; GMC, ganglion mother cell. Bar, 10 μm.

Table 5 *Hmr* and *Lhr* mutants exhibit normal chromosome alignment at metaphase

Genotype, Sex	Number of Prometaphases[a] and Metaphases	Nonaligned	Aligned	Aligned (%)
WT, control, f + m	167	70	97	58
Hmr^3, f + m	226	104	122	54
Lhr^{KO}, f + m	256	103	153	60
Hmr^3; Lhr^{KO}, f + m	182	82	100	55

[a] We considered only prometaphases with fully formed spindles (similar to metaphase spindles) with chromosomes showing the same degree of condensation as metaphase chromosomes.

hypothesize that the two proteins usually form a complex when incorporated into heterochromatin, but are partially independent when they dissociate and reassociate with heterochromatin. The results reported here agree with previous observations in embryos, showing that Lhr does not colocalize with Cid signals, or with the 359 bp and the AATAT satellite DNAs, which are both strongly fluorescent after DAPI staining (Maheshwari and Barbash 2012). However, Maheshwari and Barbash (2012) showed that, in embryonic metaphases, Lhr concentrates next to the dodecasatellite DNA that marks the third chromosome, while here we observed Hmr, but not Lhr, localization to chromosome 2 heterochromatin. These results are subject to two interpretations. It is possible that Lhr concentrates in the third chromosome heterochromatin also in brain cells, and that we failed to detect it due to differences in the fixation and/or immunostaining procedures. Alternatively, Lhr might specifically accumulate in the third chromosome heterochromatin only in embryonic cells. Regardless, the different chromosomal localizations during metaphase reinforce the conclusion that Hmr and Lhr can have partially independent localizations.

Aberrant chromosome condensation but normal centromere function in hybrid males

We next turned to an analysis of the mitotic phenotype of brains from hybrid third-instar larvae generated by crosses between *D. melanogaster* females and *D. simulans* males, in order to determine whether or not hybrids show similar phenotypes to the *D. melanogaster Hmr* and *Lhr* mutants. We first examined colchicine-treated metaphases from larval brains of viable hybrid females, and found that the chromosomes of these metaphases are morphologically indistinguishable from those of wild-type females. In addition, we found that larval brain metaphases of these females have a very low rate of CABs (<1%; Table S2), fully comparable to that of wild-type controls.

Consistent with previous results (Orr *et al.* 1997; Bolkan *et al.* 2007), hybrid male larvae displayed small brains, were devoid of imaginal discs, and had low frequencies of mitotic divisions; hybrid male cells were found to be predominantly stalled in interphase, with only a few M-phase cells escaping the interphase block (Bolkan *et al.* 2007). To define the mitotic phenotype in these hybrid brains, we first examined brain squash preparations, without colchicine and hypotonic pretreatments. This analysis revealed that hybrid male brains exhibit an about fivefold reduction of the MI compared to brains from either *D. melanogaster* or *D. simulans* third instar larvae (0.4 *vs.* 2.6 and 2.1 divisions/field observed in *D. melanogaster* and *D. simulans*, respectively); a reduction in the MI was also seen previously (Bolkan *et al.* 2007).

To evaluate chromosome condensation and integrity, we next treated hybrid male brains with hypotonic solution in the absence of colchicine pretreatment, and then immunostained preparations with an anti-phospho histone H3 (PH3) antibody that marks mitotic chromatin (Wei *et al.* 1999). We found several types of defects in chromosome structure, and none of the 100 PH3-positive cells examined appeared completely normal; 31% of mitotic cells were prophase-like cells, with elongated and poorly condensed chromosomes enriched in phospho histone H3 (Figure 8B and Figure S3). Similar cells were also observed in third-instar larval brains of *D. melanogaster* and *D. simulans* males, but, in each species, prophases accounted for ≤10% of the mitotic figures ($n > 100$ in each species). An increase in prophase-like cells in hybrids was observed previously by Bolkan *et al.* (2007). This finding suggests that, in hybrid males, prophase chromosome condensation is severely affected compared to the parent species. The hybrid male brains also showed substantial defects in chromosome condensation at later mitotic stages; 50% of dividing cells were prometaphase/metaphase figures with fuzzy chromosomes with unresolved sister chromatids. In addition, these cells often displayed obvious chromosome breaks (Figure 8C and Figure S3); 15% of the mitotic cells in hybrid male brains were prometaphases/metaphases with well-separated sister chromatids, but, in these cells, the chromosomes were fuzzy and overcondensed compared with those of the parent species. Although the hypotonic treatment reduces the frequency of anaphases (Gatti and Baker 1989), we were able to observe four anaphases (4% of the mitotic figures), which displayed a higher degree of chromosome condensation than that seen in anaphases of nonhybrid larvae from either species (Figure 8D).

To analyze mitotic divisions in a broader context, hybrid male brains not exposed to hypotonic treatment were stained for DNA, and with anti-tubulin antibodies. Dividing cells in these brains indeed form a mitotic spindle. Of the mitotic figures scored (52 excluding prophase-like figures, from 12 brains), 37% were prometaphases, 52% metaphases with well-aligned chromosomes, and 11% anaphases (Figure 9). In wild type *D. melanogaster* male brains, these mitotic figures ($n = 100$) were 36, 44, and 20% respectively; in *D. simulans*

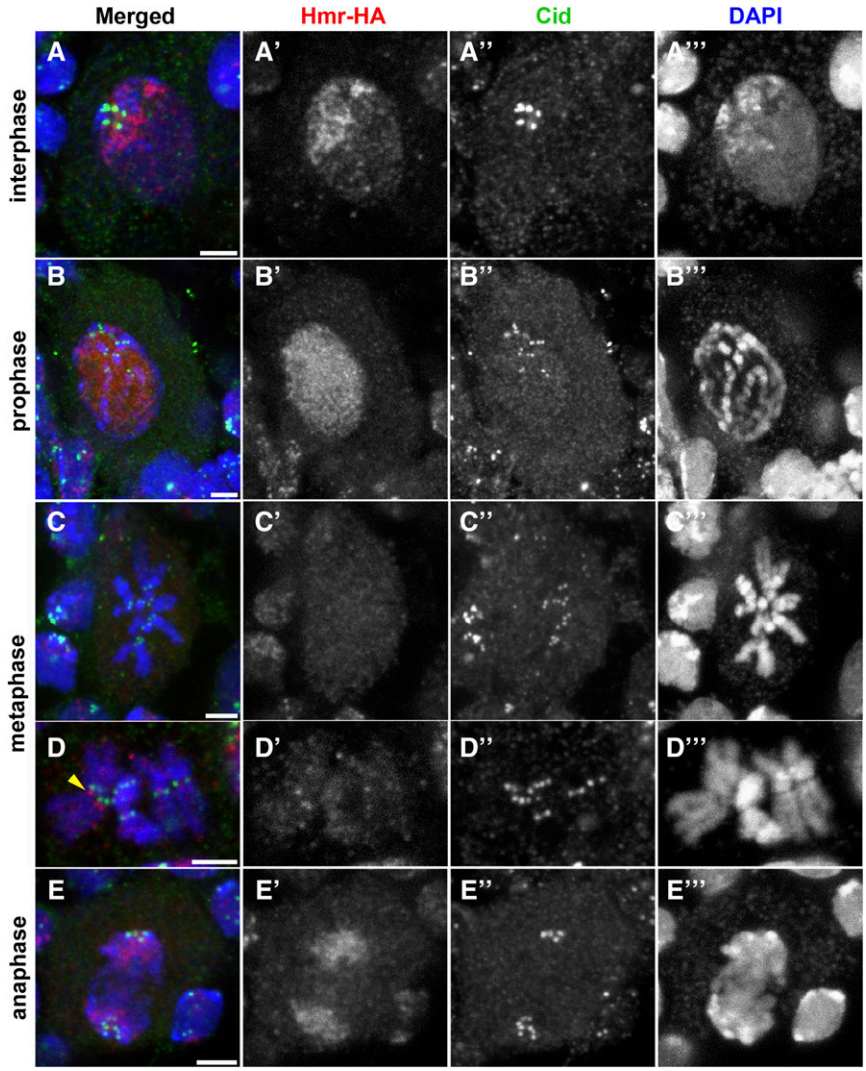

Figure 6 Localization of Hmr in male brain cells. Note the dynamic behavior of the bulk of the protein; in interphase, it is nuclear and does not colocalize with the Cid signals (A, A′, A″, A‴), it dissociates from the chromosomes during prophase (B, B′, B″, B‴) and metaphase (C, C′, C″, C‴, and D, D′, D″, D‴) and reassociates with the chromosomes during late anaphase (E, E′, E″, E‴). A fraction of metaphases showed Hmr accumulations on the 2R heterochromatin (arrowhead) (D). See text for a detailed description of the dynamic localization of Hmr. Bar, 2.5 μm.

(n = 89) they were 30, 49, and 21%, respectively. Thus, the rare dividing cells of hybrid males exhibit clear defects in chromosome condensation and integrity. However, these cells appear to have a normal centromere/kinetochore function, as suggested by the ability of the chromosomes to congregate in a metaphase plate and undergo anaphase.

Discussion

Hmr and Lhr do not have a major role in centromere function

Our data clearly show that *Hmr* and *Lhr* mutants and *Hmr*; *Lhr* double mutants exhibit very similar patterns of chromosome abnormalities. In none of the mutants did we observe hyperploid cells, which are very common in mutants that disrupt kinetochore function or the spindle checkpoint machinery (Smith *et al.* 1985; Williams *et al.* 1992, 2007). Furthermore, we found that the mutants exhibit MIs and frequencies of well-aligned metaphase plates comparable to those seen in wild-type controls. However, we discovered that the mutants have ~6% CABs, most of which were ISOBs that are likely to be generated during anaphase (Mengoli *et al.* 2014). Consistent with this idea, 15% of anaphases showed chromatin bridges, broken bridges, and/or acentric fragments caused by breaks in heterochromatin, or at the euchromatin/heterochromatin junction. Importantly, however, we never observed anaphases with intact lagging chromosomes, which indicates that the centromeres are properly aligning during metaphase, and separating during anaphase. All mutants also showed low frequencies of TFs. Thus, *Lhr* and *Hmr* mutants have a normal centromere and kinetochore function, and a weak deficiency in telomere capping, but are defective in the separation of sister chromatids during anaphase.

Previous work described Hmr and Lhr as centromere proteins. Thomae *et al.* (2013) showed S2 cell nuclei in which centromeric Cid signals were almost completely overlapping with Hmr and Lhr accumulations. However, they also showed imaginal disc cell nuclei in which several fluorescent signals generated by the centromere marker Cenp-C were not associated with Hmr and Lhr aggregates (see Figure 1 in Thomae *et al.* 2013). In addition, when Cenp-A signals were

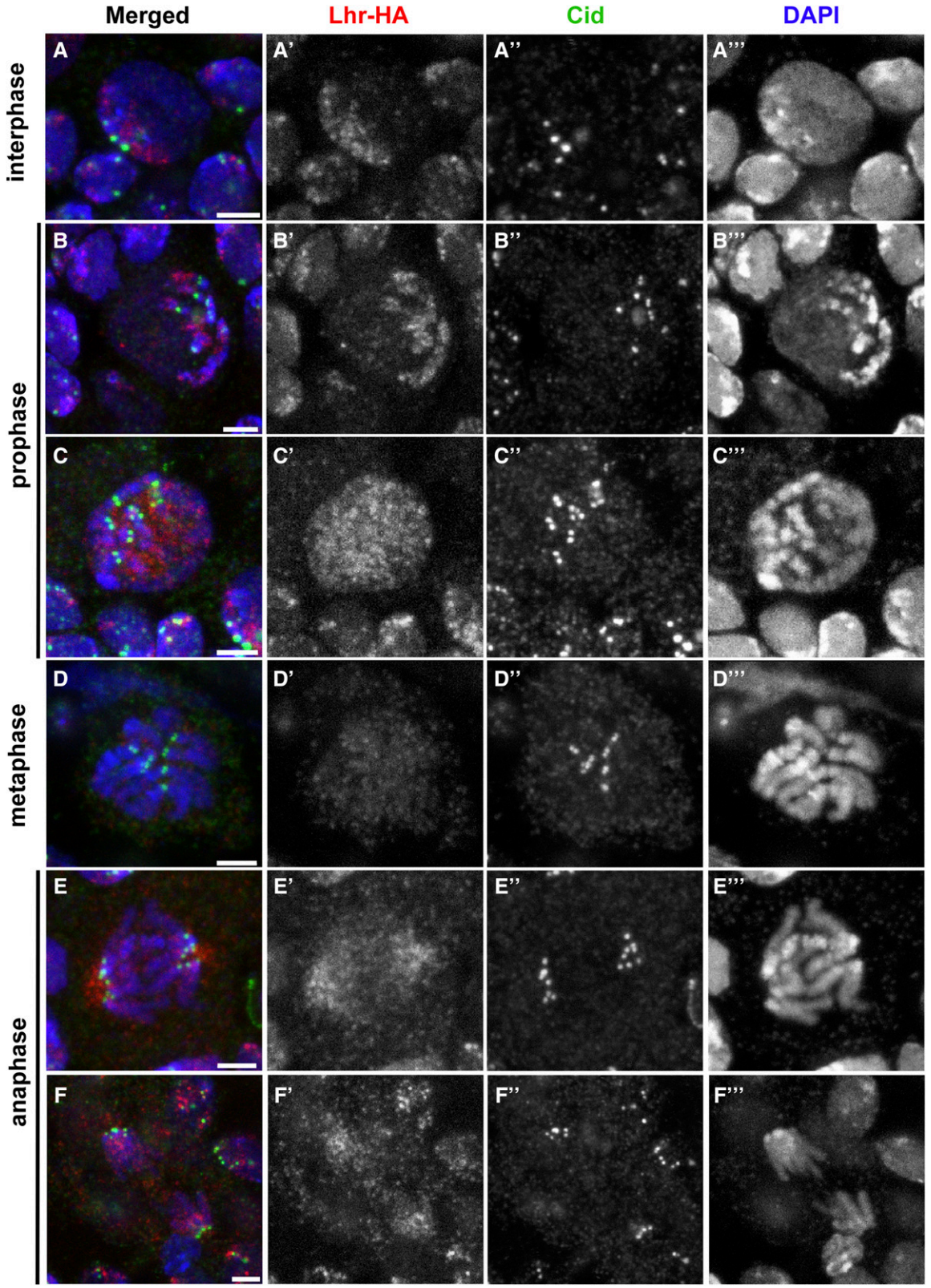

Figure 7 Localization of Lhr in male brain cells. Lhr does not colocalize with the Cid signals in interphase nuclei (A, A′, A″, A‴). Note that Lhr exhibits a dynamic behavior similar to that of Hmr (shown in Figure 6). In very early prophase, in which only heterochromatin is condensed, Lhr is still associated with the heterochromatin (B, B′, B″, B‴), but dissociates from the chromosomes in both late prophase (C, C′, C″, C‴) and metaphase (D, D′, D″, D‴) cells. Also note that, in the early anaphase shown (E, E′, E″, E‴), Lhr localizes in regions distal to the Cid signals that probably correspond to the spindle poles; in the late anaphase (F, F′, F″, F‴), Lhr is instead localized proximally to the Cid signals and is incorporated into the heterochromatin. See text for a detailed description of the dynamic localization of Lhr. Bar, 2.5 μm.

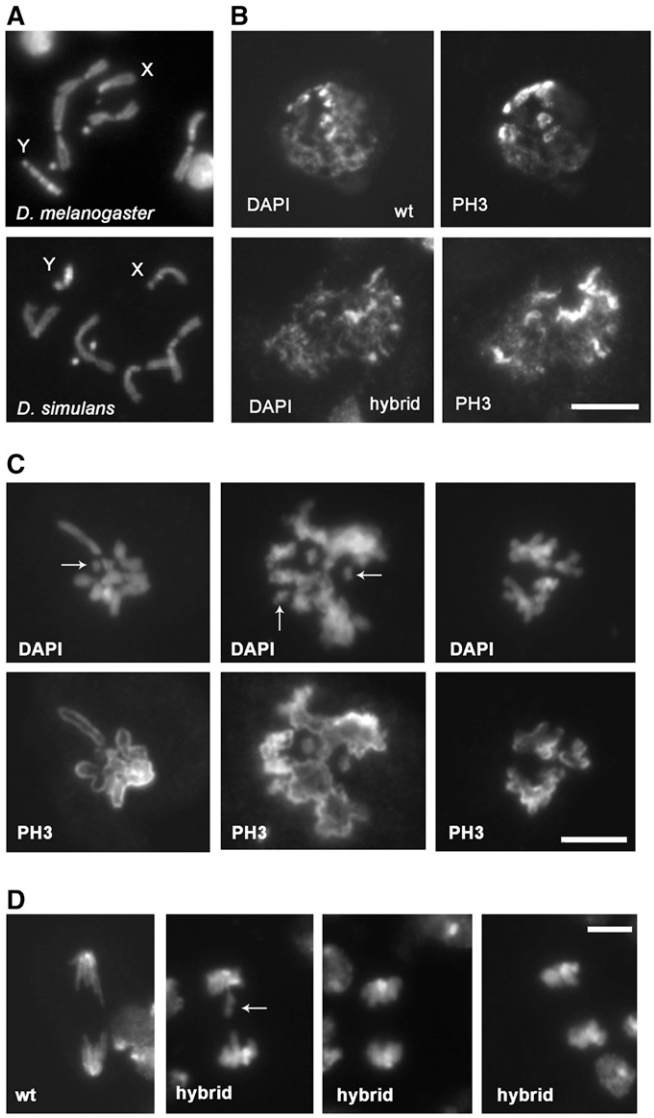

Figure 8 Hybrid males exhibit defects in chromosome condensation and integrity. Larval brains were fixed with formaldehyde, but not treated with colchicine or hypotonically swollen (see *Materials and Methods*), and then stained for DNA (DAPI) and the mitotic phospho histone H3 (PH3). (A) Male prometaphases/metaphases from wild type *D. melanogaster* and *D. simulans*; note the differences in the X chromosome heterochromatin staining and in the size of the Y chromosome. (B) Prophase-like figures from wild-type *D. melanogaster* and hybrid males. (C) Prometaphases/metaphases from hybrid males with poorly condensed and broken (arrows) chromosomes. Note that two of the cells shown (the one on the left and the central one) exhibit fuzzy chromosomes with unresolved sister chromatids. (D) Anaphases observed in wild type *D. melanogaster* and in hybrid males; note that the anaphase chromosomes in the hybrids are more condensed than in the control; one of them also exhibits a broken bridge (arrow). Bar, 5 μm.

associated with Hmr-Lhr accumulations, in many cases the two signals did not precisely colocalize, but displayed only a partial overlap. In contrast, in embryonic interphase nuclei, most Cid signals did not colocalize at all with Lhr aggregates (Maheshwari and Barbash 2012). Our analysis of Hmr and Lhr localization in interphase nuclei of larval brains showed that Hmr-HA and Lhr-HA are enriched in the chromocenter, but do not colocalize with the Cid signals. In metaphase, we found that Hmr and Lhr do not accumulate at centromeres, consistent with the observations of Thomae *et al.* (2013), though we did find that Hmr is enriched in a region of the 2R heterochromatin very close to the centromere. This observation raises the possibility that the partial overlap between the centromeric Cenp-C signals and the Hmr-Lhr signals (shown in Figure 1 of Thomae *et al.* 2013) reflects the close proximity between the centromeres and the Hmr-Lhr aggregates in pericentric heterochromatin, rather than specific accumulation of Hmr-Lhr at centromeres. We suggest that maximum intensity projections of Cid localization in S2 cells might give a different view than the confocal optical sections reported in Figure 1 of Thomae *et al.* (2013). In addition, it is possible that the differences in Hmr-Lhr localization between our study and Thomae *et al.* (2013) with respect to the centromeres reflect, at least in part, cell-specific differences in chromatin organization within the nucleus. However, the common denominator of all extant data is that not all centromeres associate with Hmr-Lhr—a finding that makes unlikely a role of Hmr-Lhr in centromere assembly or regulation.

Consistent with this conclusion, we were not able to confirm the major cytogenetic evidence reported by Thomae *et al.* (2013) for a defect in centromere function in Hmr- and Lhr-depleted cells, namely the presence of lagging chromosomes in anaphases. Although we also found lagging chromatin in mutant anaphases, Figure 2 and Figure 4 clearly demonstrate that this material consists of chromosome fragments rather than intact chromosomes. In addition, we did not observe hyperploid cells in the mutants, but instead mostly cells with ISOBs. Thus, our data argue strongly against a major functional role of Hmr and Lhr at *Drosophila* centromeres or kinetochores.

Hmr and Lhr have a role in sister chromatid separation during anaphase

One of the main questions raised by our results is the mechanism leading to the formation of aberrant anaphases in mutant cells. The main defects observed in the anaphases are continuous or broken bridges between the two daughter chromosome sets. In theory, these chromatin bridges and their broken derivatives might originate from TFs involving either sister chromatids or single nonsister chromatids. However, bridge formation from such TFs is unlikely because (i) sister TFs were never observed in either wild-type and mutant brains; and (ii) fusions between nonsister telomeres, which were present in $<1\%$ of the cells, cannot account for $\sim 15\%$ aberrant anaphases (Table 1 and Table 3). Another possible source of anaphase bridges is represented by isochromatid breaks with fusion of the proximal broken ends (sister union). The presence of a proximal sister union can only be detected in isochromatid breaks broken in euchromatin; if breaks occurred at the euchromatin–heterochromatin junction, or purely in heterochromatin, the close apposition of the proximal broken ends prevents reliable evaluation of their

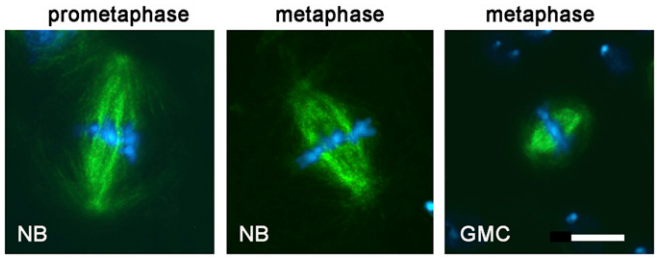

Figure 9 Hybrid males form a mitotic spindle and do not exhibit defects in chromosome alignment at metaphase. A prometaphase and two well-aligned metaphases observed in hybrid males. For control metaphases see Figure 5; NB, neuroblast; GMC, ganglion mother cell. Bar, 10 μm.

possible fusion. Two reasons, however, lead us to believe that the bridges we observe are not generated by sister union isochromatid breaks. First, we did not observe clear sister unions in the few euchromatic isochromatid breaks we detected. Second, sister union isochromatid breaks in heterochromatin are expected to give rise to very short bridges, and not to the long bridges we observed in the aberrant anaphases.

Chromatin bridges between the two anaphase chromosome sets have been also observed in *Drosophila*, chicken, and human cells depleted of condensin subunits (Steffensen *et al.* 2001; Gerlich *et al.* 2006; Green *et al.* 2012), suggesting that the phenotype observed in *Hmr* and *Lhr* mutant brains may be caused by a primary defect in sister chromatid separation (Figure 3). Sister chromatid separation is a complex process that involves three major players: the cohesin and condensin multiprotein complexes, and topoisomerase II. Cohesin is required for holding sister chromatids together after DNA replication, while condensin ensures proper chromosome structure and separation of sister chromatids during anaphase (reviewed by Hirano 2015; Uhlmann 2016). Topoisomerase II decatenates the DNA molecules of the two sister chromatids; it has also been posited that condensin is required for the organization of a correct axial chromatid structure in which topoisomerase II can efficiently promote sister chromatid decatenation (Coelho *et al.* 2003; reviewed by Hirano 2015; Uhlmann 2016). Accordingly, mutations in the *Drosophila* condensin subunit genes *gluon* (SMC4), *barren* (CAP-H), *Cap-D2*, and *Cap-G* result in abnormally condensed chromosomes and formation of extensive chromatin bridges at anaphase (Bhat *et al.* 1996; Steffensen *et al.* 2001; Dej *et al.* 2003; Somma *et al.* 2003; Savvidou *et al.* 2005). Anaphase bridges have also been observed in *Drosophila* S2 cells depleted of Topoisomerase II (Chang *et al.* 2003; Coelho *et al.* 2008; Somma *et al.* 2008), and in *Top2* mutant brains (Mengoli *et al.* 2014). Condensins associate with chromatin during S phase and remain bound to the chromosomes during G2 and prophase; after nuclear envelope breakdown, additional condensin subunits are recruited to prometaphase chromosomes (reviewed by Hirano 2015). In contrast, the bulk of cohesin is released from the chromosomes during prophase and returns to the chromosomes during anaphase-telophase. A fraction of cohesin remains bound to the centromeric regions, and, in very small amounts, also to the noncentromeric regions of prometaphase and metaphase chromosomes; centromeric cohesin is then cleaved by separase to allow sister chromatid separation at the onset of anaphase (Warren *et al.* 2000; reviewed by Dorsett and Ström 2012; Hirano 2015; Uhlmann 2016). Thus, the Hmr and Lhr chromosome association/dissociation behavior is similar to cohesins, but Hmr and Lhr are required for proper sister chromatid separation like condensins.

At this stage, we can only speculate about the primary defect in sister chromatid separation leading to chromatin bridges in the mutants. The findings that, in *Hmr* and *Lhr* mutants, metaphase chromosomes are morphologically normal, and anaphase and metaphase defects are ranging from 12 to 16.5%, suggest that potential variation in condensin or Top2 levels would be minimal and difficult to detect. It is also unlikely that these defects are caused by a direct or indirect defect in Top2 function, because brains from larvae bearing weak mutations in the *Top2* gene exhibit a highly specific pattern of incomplete aberrations, involving specific regions of the Y chromosome and a single region of 3L heterochromatin (region 47) (Mengoli *et al.* 2014). In contrast, in *Hmr* and *Lhr* mutants, we observed breaks in both 3L and 3R heterochromatin, and in the second chromosome heterochromatin. Thus, we favor the possibility that the anaphase bridges observed in *Hmr* and *Lhr* mutant cells result from an aberrant sister chromatid attachment established during interphase that becomes phenotypically manifest when cells enter anaphase.

Regardless of the underlying mechanism, our observations raise the question of why most complete ISOBs are broken at the euchromatin-heterochromatin junctions. The transition between heterochromatin and euchromatin appears to be gradual, rather than abrupt, in terms of DNA content. The junctions do not contain specific DNA sequences, and are instead mosaics of middle-repetitive DNA interspersed with single-copy DNA (Miklos and Cotsell 1990; Hoskins *et al.* 2002). However, there is an obvious change in DNA fiber compaction at the euchromatin–heterochromatin transition that might render these regions prone to breakage when chromatin bridges are pulled by the spindle (Miklos and Cotsell 1990). To the best of our knowledge, the literature about preferential sites for anaphase bridge rupture is rather limited. *In vivo* analysis of human cancer cells containing marked repeated DNA inserted into the chromosomes showed that bridges are preferentially severed at sites near the inserted DNA (Shimizu *et al.* 2005). In addition, in fixed cells from embryogenic callus cultures, most breakages of anaphase bridges occurred within heterochromatic knobs, or at the junction between euchromatin and the knobs (Fluminhan and Kameya 1996). These reports support the hypothesis that euchromatin–heterochromatin transition regions in anaphase bridges are more prone to breakage than

euchromatic regions when pulled by spindle-generated forces.

Do hybrids have a mitotic defect similar to the Hmr and Lhr phenotype in D. melanogaster?

Our results strongly suggest that loss of the Lhr-Hmr complex in *D. melanogaster* results in abnormal adhesion between sister chromatids, which leads to anaphase bridges and chromosome breakage. The lethality of interspecific hybrids, however, results from the presence of wild-type *Hmr* and *Lhr*, not their loss. We therefore re-examined the chromosomal phenotype of dying hybrid males to investigate whether or not it shows any similarity to *Hmr* and *Lhr D. melanogaster* mutants. The detectable but nonessential roles of *Hmr* and *Lhr* in fundamental functions such as the control of transposition, telomere homeostasis, and sister chromatid separation suggest that these genes might play redundant functions in some essential processes, but may or may not offer insight into why mutations in *Hmr* and *Lhr* suppress hybrid male lethality. This uncertainty reflects what may be a general property of hybrid incompatibility genes: hybrid phenotypes often represent a gain-of-function because they are caused by the presence of wild-type alleles, while the intraspecific phenotypes are typically discovered and analyzed using loss-of-function mutations (Maheshwari and Barbash 2011).

Previous research showed that most brain cells of hybrid males are arrested in either the G1 or G2 phase and rarely enter mitosis (Bolkan *et al.* 2007). It has also been reported that a fraction of these cells exhibits highly aberrant chromatin morphology, suggesting that they represent mitotic cells with severely undercondensed chromosomes (Orr *et al.* 1997). Furthermore, it has been suggested that hybrid male cells have some form of chromatin defect specific to the X chromosome—a hypothesis supported by interactions between dosage compensation mutations and hybrid viability (Barbash 2010). It is challenging to determine if hybrids show a phenotype comparable, at least in part, to that seen in *Hmr* and *Lhr* mutants, due to the relatively low penetrance of these mutant phenotypes in *D. melanogaster* and the low frequency of mitotic cells in hybrids. We were able to image sufficient mitotic cells in hybrids to conclude that chromosomes align properly during metaphase. Based on this result, and the small number of anaphases observed, there is no evidence that hybrid lethality results from centromere or kinetochore dysfunction (Figure 9). We did, however, identify defects in chromosome condensation and integrity in hybrid males that are reminiscent of those observed in cells depleted of condensins or showing abnormal accumulations of cohesins (Figure 8) (Bhat *et al.* 1996; Steffensen *et al.* 2001; Dej *et al.* 2003; Somma *et al.* 2003; Cobbe *et al.* 2006; Savvidou *et al.* 2005; Oliveira *et al.* 2014). Interestingly, these defects have been shown to interfere with sister chromatid separation leading to anaphase bridges. It will therefore be of interest in future studies to determine whether *Hmr* and *Lhr* mutants and interspecific hybrids have altered distributions and functional defects in condensins, cohesins, or cohesin loading/releasing factors.

Acknowledgments

We thank Dean Castillo, Anne-Marie Dion-Côté, Michael Goldberg, and Sarah Sander for helpful comments on the manuscript. J.A.B. was the recipient of a student grant from the United States–Italy Fulbright Commission. Y.M.Y. is supported by the Howard Hughes Medical Institute. This work was supported in part by a Research Projects of National Interest/Italian Ministry of Education, Universities and Research (PRIN/MIUR) grant to S.B., a grant from Associazione Italiana per la Ricerca sul Cancro (IG 16020) to M.G., and by National Institutes of Health (NIH) R01GM074737 to D.A.B.

Literature Cited

Alekseyenko, A. A., A. A. Gorchakov, B. M. Zee, S. M. Fuchs, P. V. Kharchenko *et al.*, 2014 Heterochromatin-associated interactions of Drosophila HP1a with dADD1, HIPP1, and repetitive RNAs. Genes Dev. 28: 1445–1460.

Aruna, S., H. A. Flores, and D. A. Barbash, 2009 Reduced fertility of Drosophila melanogaster hybrid male rescue (Hmr) mutant females is partially complemented by Hmr orthologs from sibling species. Genetics 181: 1437–1450.

Barbash, D. A., 2010 Genetic testing of the hypothesis that hybrid male lethality results from a failure in dosage compensation. Genetics 184: 313–316.

Benna, C., S. Bonaccorsi, C. Wulbeck, C. Helfrich-Forster, M. Gatti *et al.*, 2010 Drosophila timeless2 is required for chromosome stability and circadian photoreception. Curr. Biol. 20: 346–352.

Bhat, M. A., A. V. Philp, D. M. Glover, and H. J. Bellen, 1996 Chromatid segregation at anaphase requires the barren product, a novel chromosome-associated protein that interacts with topoisomerase II. Cell 87: 1103–1114.

Bolkan, B. J., R. Booker, M. L. Goldberg, and D. A. Barbash, 2007 Developmental and cell cycle progression defects in Drosophila hybrid males. Genetics 177: 2233–2241.

Bonaccorsi, S., M. G. Giansanti, and M. Gatti, 2000 Spindle assembly in Drosophila neuroblasts and ganglion mother cells. Nat. Cell Biol. 2: 54–56.

Cenci, G., R. B. Rawson, G. Belloni, D. H. Castrillon, M. Tudor *et al.*, 1997 UbcD1, a Drosophila ubiquitin-conjugating enzyme required for proper telomere behavior. Genes Dev. 11: 863–875.

Chang, H.-J., S. Goulding, W. C. Earnshaw, and M. Carmena, 2003 RNAi analysis reveals an unexpected role for topoisomerase II in chromosome arm congression to a metaphase plate. J. Cell Sci. 116: 4715–4726.

Cicconi, A., E. Micheli, F. Vernì, A. Jackson, A. C. Gradilla *et al.*, 2017 The Drosophila telomere-capping protein Verrocchio binds single-stranded DNA and protects telomeres from DNA damage response. Nucleic Acids Res. 45: 3068–3085.

Cobbe, N., E. Savvidou, and M. M. Heck, 2006 Diverse mitotic and interphase functions of condensins in Drosophila. Genetics 172: 991–1008.

Coelho, P. A., J. Queiroz-Machado, and C. E. Sunkel, 2003 Condensin-dependent localisation of topoisomerase II to an axial chromosomal structure is required for sister chromatid resolution during mitosis. J. Cell Sci. 116: 4763–4776.

Coelho, P. A., J. Queiroz-Machado, A. M. Carmo, S. Moutinho-Pereira, H. Maiato *et al.*, 2008 Dual role of topoisomerase II in centromere resolution and aurora B activity. PLoS Biol. 6: e207.

Dej, K. J., C. Ahn, and T. L. Orr-Weaver, 2003 Mutations in the Drosophila condensin subunit dCAP-G: defining the role of condensin for chromosome condensation in mitosis and gene expression in interphase. Genetics 168: 895–906.

Dorsett, D., and L. Ström, 2012 The ancient and evolving roles of cohesin in gene expression and DNA repair. Curr. Biol. 22: R240–R250.

Durante, M., J. S. Bedford, D. J. Chen, S. Conrad, M. N. Cornforth *et al.*, 2013 From DNA damage to chromosome aberrations: joining the break. Mutat. Res. 756: 5–13.

Elgin, S. C., and G. Reuter, 2013 Position-effect variegation, heterochromatin formation, and gene silencing in Drosophila. Cold Spring Harb. Perspect. Biol. 5: a017780.

Fanti, L., G. Giovinazzo, M. Berloco, and S. Pimpinelli, 1998 The heterochromatin protein 1 prevents telomere fusions in Drosophila. Mol. Cell 2: 527–538.

Fluminhan, A., and T. Kameya, 1996 Behaviour of chromosomes in anaphase cells in embryogenic callus cultures of maize (Zea mays L.). Theor. Appl. Genet. 92: 982–990.

Gatti, M., 1979 Genetic control of chromosome breakage and rejoining in Drosophila melanogaster: spontaneous chromosome aberrations in X-linked mutants defective in DNA metabolism. Proc. Natl. Acad. Sci. USA 76: 1377–1381.

Gatti, M., and B. S. Baker, 1989 Genes controlling essential cell cycle functions in Drosophila melanogaster. Genes Dev. 3: 438–453.

Gatti, M., and M. L. Goldberg, 1991 Mutations affecting cell division in Drosophila. Methods Cell Biol. 35: 543–586.

Gatti, M., and S. Pimpinelli, 1992 Functional elements in Drosophila melanogaster heterochromatin. Annu. Rev. Genet. 26: 239–275.

Gatti, M., C. Tanzarella, and G. Olivieri, 1974 Analysis of the chromosome aberrations induced by x-rays in somatic cells of Drosophila melanogaster. Genetics 77: 701–719.

Gerlich, D., T. Hirota, B. Koch, J. M. Peters, and J. Ellenberg, 2006 Condensin I stabilizes chromosomes mechanically through a dynamic interaction in live cells. Curr. Biol. 21: 333–344.

Green, L. C., P. Kalitsis, T. M. Chang, M. Cipetic, J. H. Kim *et al.*, 2012 Contrasting roles of condensin I and condensin II in mitotic chromosome formation. J. Cell Sci. 125: 1591–1604.

Greil, F., E. de Wit, H. J. Bussemaker, and B. van Steensel, 2007 HP1 controls genomic targeting of four novel heterochromatin proteins in Drosophila. EMBO J. 26: 741–751.

Heeger, S., O. Leismann, R. Schittenhelm, O. Schraidt, S. Heidmann *et al.*, 2005 Genetic interactions of separase regulatory subunits reveal the diverged Drosophila Cenp-C homolog. Genes Dev. 19: 2041–2053.

Hirano, T., 2015 Chromosome dynamics during mitosis. Cold Spring Harb. Perspect. Biol. 7: a015792.

Hoskins, R. A., C. D. Smith, J. W. Carlson, A. B. Carvalho, A. Halpern *et al.*, 2002 Heterochromatic sequences in a Drosophila whole-genome shotgun assembly. Genome Biol. 3: RESEARCH0085.

Joppich, C., S. Scholz, G. Korge, and A. Schwendemann, 2009 Umbrea, a chromo shadow domain protein in Drosophila melanogaster heterochromatin, interacts with Hip, HP1and HOAP. Chromosome Res. 17: 19–36.

Lattao, R., S. Bonaccorsi, X. Guan, S. A. Wasserman, and M. Gatti, 2011 Tubby-tagged balancers for the Drosophila X and second chromosomes. Fly (Austin) 5: 369–370.

Maheshwari, S., and D. A. Barbash, 2011 The genetics of hybrid incompatibilities. Annu. Rev. Genet. 45: 331–355.

Maheshwari, S., and D. A. Barbash, 2012 Cis-by-trans regulatory divergence causes the asymmetric lethal effects of an ancestral hybrid incompatibility gene. PLoS Genet. 8: e1002597.

Marzio, A., C. Merigliano, M. Gatti, and F. Vernì, 2014 Sugar and chromosome stability: clastogenic effects of sugars in vitamin B6-deficient cells. PLoS Genet. 10: e1004199.

Mengoli, V., E. Bucciarelli, R. Lattao, R. Piergentili, M. Gatti *et al.*, 2014 The analysis of mutant alleles of different strength reveals multiple functions of topoisomerase 2 in regulation of Drosophila chromosome structure. PLoS Genet. 10: e1004739.

Merigliano, C., A. Marzio, F. Renda, M. P. Somma, M. Gatti *et al.*, 2017 A role for the twins protein phosphatase (PP2A–B55) in the maintenance of Drosophila genome integrity. Genetics 205: 1151–1167.

Miklos, G. L., and J. N. Cotsell, 1990 Chromosome structure at interfaces between major chromatin types: alpha- and beta-heterochromatin. Bioessays 12: 1–6.

Obe, G., P. Pfeiffer, J. R. Savage, C. Johannes, W. Goedecke *et al.*, 2002 Chromosomal aberrations: formation, identification and distribution. Mutat. Res. 504: 17–36.

Oliveira, R. A., S. Kotadia, A. Tavares, M. Mirkovic, K. Bowlin *et al.*, 2014 Centromere-independent accumulation of cohesin at ectopic heterochromatin sites induces chromosome stretching during anaphase. PLoS Biol. 12: e1001962.

Orr, H. A., L. D. Madden, J. A. Coyne, R. Goodwin, and R. S. Hawley, 1997 The developmental genetics of hybrid inviability: a mitotic defect in Drosophila hybrids. Genetics 145: 1031–1040.

Presgraves, D. C., 2010 The molecular evolutionary basis of species formation. Nat. Rev. Genet. 11: 175–180.

Raffa, G. D., G. Siriaco, S. Cugusi, L. Ciapponi, G. Cenci *et al.*, 2009 The Drosophila modigliani (moi) gene encodes a HOAP-interacting protein required for telomere protection. Proc. Natl. Acad. Sci. USA 106: 2271–2276.

Raffa, G. D., D. Raimondo, C. Sorino, S. Cugusi, G. Cenci *et al.*, 2010 Verrocchio, a Drosophila OB fold-containing protein, is a component of the terminin telomere-capping complex. Genes Dev. 24: 1596–1601.

Ross, B. D., L. Rosin, A. W. Thomae, M. A. Hiatt, D. Vermaak *et al.*, 2013 Stepwise evolution of essential centromere function in a Drosophila neogene. Science 340: 1211–1214.

Satyaki, P. R., T. N. Cuykendall, K. H. Wei, N. J. Brideau, H. Kwak *et al.*, 2014 The Hmr and Lhr hybrid incompatibility genes suppress a broad range of heterochromatic repeats. PLoS Genet. 10: e1004240.

Savvidou, E., N. Cobbe, S. Steffensen, S. Cotterill, and M. M. Heck, 2005 Drosophila CAP-D2 is required for condensin complex stability and resolution of sister chromatids. J. Cell Sci. 118: 2529–2543.

Shimizu, N., K. Shingaki, Y. Kaneko-Sasaguri, T. Hashizume, and T. Kanda, 2005 When, where and how the bridge breaks: anaphase bridge breakage plays a crucial role in gene amplification and HSR generation. Exp. Cell Res. 302: 233–243.

Smith, D. A., B. S. Baker, and M. Gatti, 1985 Mutations in genes encoding essential mitotic functions in Drosophila melanogaster. Genetics 110: 647–670.

Somma, M. P., B. Fasulo, G. Siriaco, and G. Cenci, 2003 Chromosome condensation defects in barren RNA-interfered Drosophila cells. Genetics 165: 1607–1611.

Somma, M. P., F. Ceprani, E. Bucciarelli, V. Naim, V. De Arcangelis *et al.*, 2008 Identification of Drosophila mitotic genes by combining co-expression analysis and RNA interference. PLoS Genet. 4: e1000126.

Steffensen, S., P. A. Coelho, N. Cobbe, S. Vass, M. Costa *et al.*, 2001 A role for Drosophila SMC4 in the resolution of sister chromatids in mitosis. Curr. Biol. 11: 295–307.

Thomae, A. W., G. O. Schade, J. Padeken, M. Borath, I. Vetter *et al.*, 2013 A pair of centromeric proteins mediates reproductive isolation in Drosophila species. Dev. Cell 27: 412–424.

Uhlmann, F., 2016 SMC complexes: from DNA to chromosomes. Nat. Rev. Mol. Cell Biol. 7: 399–412.
Vermaak, D., and H. S. Malik, 2009 Multiple roles for heterochromatin protein 1 genes in Drosophila. Annu. Rev. Genet. 43: 467–492.
Warren, W. D., S. Steffensen, E. Lin, P. Coelho, M. Loupart *et al.*, 2000 The Drosophila RAD21 cohesin persists at the centromere region in mitosis. Curr. Biol. 10: 1463–1466.
Wei, Y., L. Yu, J. Bowen, M. A. Gorovsky, and C. D. Allis, 1999 Phosphorylation of histone H3 is required for proper chromosome condensation and segregation. Cell 97: 99–109.
Williams, B. C., T. L. Karr, J. M. Montgomery, and M. L. Goldberg, 1992 The Drosophila l(1)zw10 gene product, required for accurate mitotic chromosome segregation, is redistributed at anaphase onset. J. Cell Biol. 118: 759–773.
Williams, B. G., H. Leung, A. Maiato, Z. Wong, Z. Li *et al.*, 2007 Mitch a rapidly evolving component of the Ndc80 kinetochore complex required for correct chromosome segregation in Drosophila. J. Cell Sci. 120: 3522–3533.
Zhang, Y., L. Zhang, X. Tang, S. R. Bhardwaj, J. Ji *et al.*, 2016 MTV, an ssDNA protecting complex essential for transposon-based telomere maintenance in Drosophila. PLoS Genet. 12: e1006435.

Communicating editor: J. Sekelsky